

## 厚生労働科学研究費補助金（創薬基盤推進研究事業）

### 分担研究報告書

新規創薬を目指した生活習慣病・難治性疾患モデル遺伝子変異ラットの開発と解析

－高血圧、腎臓病モデル遺伝子変異ラット開発と解析－

分担研究者：横井 秀基

京都大学大学院医学研究科 内分泌代謝内科 助教

**研究要旨** 本研究課題は、新規開発した標的遺伝子変異ラット開発システムを用いて、生活習慣病や難治性疾患に関連する複数の遺伝子変異ラットを開発し、新規生活習慣病・難治性疾患モデルラットを樹立し、従来マウスにおいて実施・解析が困難であった系統的な生理学的解析、移植実験、薬理薬効評価解析などの施行を容易にする事により、生活習慣病関連疾患、難治性疾患の病態解明、新規治療標的の同定および創薬開発を加速させることを目的とする。本年度は、昨年度までに新規遺伝子変異ラット樹立技術を用いて、高血圧、腎臓病に関連した生活習慣病・難治性疾患関連遺伝子変異ラットのスクリーニングを行った結果得られた、ナトリウム利尿ペプチド受容体遺伝子のミスセンス変異体を有する遺伝子変異ラットの解析を行った。

#### A. 研究目的

現在生活習慣病関連疾患である心筋梗塞、心不全、糖尿病、脳卒中、慢性腎臓病（CKD）などの病態解明、新規治療標的の同定に基づく新規治療薬、治療法開発が望まれている。現在これら疾患の病態解析、創薬開発、再生医療研究には遺伝子改変技術が確立されているマウスがモデル動物として多く用いられているが、マウスはその小ささゆえに採血や組織採取（脾臓、中枢神経系）が困難であること、生理学的解析や移植実験が行ないにくいなどの問題がある。さらに、最近では代謝面においてヒトと大きく異なる生理的特徴が明らかとなった

(Vassilopoulos, et al. Science 2009)。そのため、マウスと比べ体のサイズが大きく、採血や組織採取や系統的な生理学的解析が容易で、移植実験も行ないやすく、代謝面でもよりヒトに近いラットでの疾患モデル確立が期待されている。しかし、現時点ではES細胞の技術がラットで未確立のため、遺伝子改変ラットの効率的な作成は不可能である。最近、京都大学の芹川、真下らが、ENUミュータジェネシスに、新規DNAスクリーニング法（MuT-power）、凍結精子アーカイブからの個体復元技術（ICSI）という一連の新規技術を組み合わせることにより、標的遺伝子変異ラットの効率的な作成システム構築に成功した。本研究課題では、このシステムを用いて生活習慣病関連・難治性疾患遺伝子変異ラットをスクリーニングし、その表現系を解析することにより高血圧、CKDなどの新

規生活習慣病モデルラットを開発し、その詳細な解析を通して病態解明、新規治療標的の同定を行なうと共に、このモデルを用いた新規創薬開発を加速させることを目的とする。

#### B. 研究方法

昨年度までに、生活習慣病・難治性疾患関連遺伝子に関するENUミュータジェネシスによる約1600匹分のラットミュータントアーカイブの高速DNAスクリーニングを行った。候補遺伝子としては高血圧モデルとしてナトリウム利尿ペプチド関連遺伝子、腎臓病としてpodocin, TRPC6遺伝子などをスクリーニングした。具体的にはそれぞれの標的遺伝子のcoding領域に対応するprimer setを作製し、ENUミュータジェネシスを行なったラットの遺伝子アーカイブから新規変異DNAスクリーニング法（MuT-POWER法）を用いてスクリーニングを行なった。この方法はDNAミスマッチ部位に特異的かつ短時間に挿入されるトランスポゾンMuの性質を利用し、さらにプール法および蛍光標識DNAを組み合わせることにより短時間かつ低コストで変異DNAのスクリーニング、変異ラットの同定を可能としたものである。このスクリーニングにより候補遺伝子の変異が見つかった場合は新規開発した個体復元技術ICSIを用いて標的遺伝子変異ラットを樹立した。これらの過程はひとつの遺伝子のスクリーニング開始から、変異の同定、変異ラットの樹立までおよそ6ヶ月から1年で行なうことが可能

である。

本年度はこうしたスクリーニングにより得られ、系統樹立した、ナトリウム利尿ペプチド受容体遺伝子のミスセンス変異体ラットの解析を中心におこなった。具体的には本ラットの血圧、尿中cGMP濃度の測定などを行い、本ラットのモデルラットとしての意義を解析した。

またこれら実験動物を用いる研究に際しては「動物の愛護および管理に関する法律」（平成17年6月改正法）、「京都大学における動物実験の実施に関する規程」および「京都大学大学院医学研究科・医学部における動物実験の実施に関する規程」（いずれも平成19年4月改訂）を遵守して実施し、動物に与える苦痛を最小限にとどめるように最善の配慮を尽くしている。

### C. 研究結果

本年度は、生活習慣病・難治性疾患関連遺伝子に関するENUミュータジェネシスによる約1600匹分のラットミュータントアーカイブの高速DNAスクリーニングの結果得られた、ナトリウム利尿ペプチド1型受容体遺伝子(GC-A)のミスセンス変異を有するラット(GC-A変異ラット)の系統樹立を行い、その解析を行った。このラットはナトリウム利尿ペプチド1型受容体の guanylyl cyclase domain に変異を有し、その活性の低下が予想された。GC-A変異ラットは野生型ラットと比べ特に体重や成長には差がなかったが、血圧を測定したところ、血圧が高い傾向が特に雌において示された。現在さらに数を増やして解析を継続している。またこの変異が機能的変異であることをより直接的に確認するためにGC-A変異ラットにANPを静脈内注射し、その血圧および尿中cGMP濃度を前後で測定し、比較検討を開始した。今後さらにこれら表現系解析を継続する予定である。

### D. 考察

生活習慣病関連疾患の病態解明においては複数の臓器における病態の同時進行的変化とそれに伴う液性因子を介した臓器間シグナルクロストーク解明が必須であり、またこれら病態には細胞老化も関与するため、その治療において細胞・臓器再生という観点も不可欠である。現在これら疾患の病態解析、創薬開発、再生医

療研究には遺伝子改変技術が確立されているマウスがモデル動物として多く用いられているが、マウスはその小ささゆえに採血や組織採取が困難であること、生理学的解析や移植実験が行ないにくいなどの問題がある。そのため、マウスと比べ体のサイズが大きく、採血や組織採取や系統的な生理学的解析が容易で、移植実験も行ないやすく、代謝面でもよりヒトに近いラットでの疾患モデル確立が期待されている。今回、心臓ホルモンであるナトリウム利尿ペプチドの受容体である GC-A にミスセンス変異を有する GC-A 変異ラットの作製とその系統樹立に成功し、その解析を開始した。今後、本ラットのさらなる解析が生活習慣病などの病態解明に役立つと共に、そのモデル動物としての利用が、新規治療標的の同定および新規創薬開発につながることを期待し、研究を継続している。

### E. 結論

生活習慣病・難治性疾患関連遺伝子に関して、ENUミュータジェネシスによる約1600匹分のラットミュータントアーカイブの高速DNAスクリーニングを行い、ナトリウム利尿ペプチド1型受容体遺伝子に変異を有するラットの作製に成功した。今後、本研究にて得られたナトリウム利尿ペプチド1型受容体(GC-A)遺伝子変異ラットの表現系を解析し、疾患モデルラットとしての意義を確立し、病態解明・新規治療標的の同定と新規創薬開発を加速させる予定である。

### F. 健康危険情報

なし

### G. 研究発表

#### 1. 論文発表

1. Yokoi, H., Kasahara, M., Mori, K., Kuwabara, T., Toda, N., Yamada, R., Namoto, S., Yamamoto, T., Seki, N., Souma, N., Yamaguchi, T., Sugawara, A., Mukoyama, M., and Nakao, K. Peritoneal fibrosis and high transpoare induced in mildly pre-injured peritoneum by 3,4-dideoxyglucosone-3-ene in mice. *Perit. Dial. Int.* 33:143-154, 2013.
2. Ogawa, Y., Mukoyama, M., Yokoi, H., Kasahara, M., Mori, K., Kato, Y., Kuwabara, T., Imamaki, H., Kawanishi, T., Koga, K., Ishii, A., Tokudome, T., Kishimoto, I., Sugawara, A., Nakao, K. Natriuretic peptide receptor guanylyl cyclase-A protects

- podocytes from aldosterone-induced glomerular injury. *J. Am. Soc. Nephrol.* 23:1198-1209, 2012.
3. Yokoi, H., Kasahara, M., Mori, K., Ogawa, Y., Kuwabara, T., Imamaki, H., Kawanishi, T., Koga, K., Ishii, A., Kato, Y., Mori, P. K., Toda, N., Ohno, S., Muramatsu, H., Muramatsu, T., Sugawara, A., Mukoyama, M., and Nakao, K. Pleiotrophin triggers inflammation and increased peritoneal permeability leading to peritoneal fibrosis. *Kidney Int.* 81, 160-169, 2012.
  4. Kuwabara, T., Mori, K., Mukoyama, M., Kasahara, M., Yokoi, H., Saito, Y., Ogawa, Y., Imamaki, H., Kawanishi, T., Ishii, A., Koga, K., Mori, P.K., Kato, Y., Sugawara, A., Nakao, K. Exacerbation of diabetic nephropathy by hyperlipidaemia is mediated by toll-like receptor 4 in mice. *Diabetologia* 55:2256-2266, 2012.
2. 学会発表  
国際学会
1. Y.Kato, M.Mukoyama, H.Yokoi, Y.Ogawa, K.Mori, M.Kasahara, T.Kuwabara, H.Imamaki, T.Kawanishi, K.Nakao  
Role of p38 mapk in aldosterone-induced glomerular injury in natriuretic peptide receptor-a deficient mice  
Hypertension Sydney 2012  
Sep 30-Oct 4, 2012 Sydney
  2. T.Kuwabara, K.Mori, M.Mukoyama, M.Kasahara, H.Yokoi, H.Imamaki, A.Ishii, K.Koga, K.P.Mori, Y.Kato, N.Toda, S.Ono, A.Sugawara, K.Nakao  
Macrophage-mediated glucolipotoxicity contributes to progression of diabetic nephropathy through MRP8/TLR4 signaling  
American Society of Nephrology  
Nov 3 (Oct 30 - Nov 4), 2012 San Diego
  3. Ishii, H.Imamaki, K.Mori, M.Mukoyama, H.Yokoi, M.Kasahara, T.Kuwabara, Y.Ogawa, T.Kawanishi, K.Koga, K.P.Mori, Y.Kato, N.Toda, S.Ono, A.Sugawara, K.Nakao  
Role of kidney injury biomarker Ngal in obesity and energy homeostasis  
American Society of Nephrology  
Oct 30 - Nov 4, 2012 San Diego
  4. K.Koga, M.Mukoyama, H.Yokoi, K.Mori, M.Kasahara, T.Kuwabara, H.Imamaki, T.Kawanishi, A.Ishii, K.P.Mori, Y.Kato, S.Ono, N.Toda, Moin A. Saleem, A.Sugawara, K.Nakao  
microRNA-26a is upregulated in glomeruli of diabetic mice and attenuates TGFβ1-induced extracellular matrix expression in podocytes by inhibiting both CTGF and SMAD2  
American Society of Nephrology  
Nov 1 (Oct 30 - Nov 4), 2012 San Diego
  5. K.Koga, M.Mukoyama, H.Yokoi, M.Kasahara, T.Kuwabara, H.Imamaki, T.Kawanishi, A.Ishii, K.P.Mori, Y.Kato, S.Ono, N.Toda, A.Sugawara, K.Nakao  
Analyses of microRNAs targeting CTGF in peritoneal fibrosis mouse model  
American Society of Nephrology  
Nov 2 (Oct 30 - Nov 4), 2012 San Diego
  6. K.P.Mori, M.Mukoyama, H.Yokoi, M.Kasahara, T.Kuwabara, H.Imamaki, Y.Ogawa, T.Kawanishi, A.Ishii, K.Koga, Y.Kato, N.Toda, S.Ono, A.Sugawara, K.Nakao  
Alteration of renal lipid deposition and gene expression induced by fasting and high-fat diet feeding  
American Society of Nephrology  
Nov 3 (Oct 30 - Nov 4), 2012 San Diego
  7. K.P.Mori, K.Mori, M.Mukoyama, H.Yokoi, M.Kasahara, T.Kuwabara, H.Imamaki, A.Ishii, K.Koga, Y.Kato, A.Sugawara, T.Endo, M.Yanagita, K.Nakao  
Acute disruption of megalin expression in renal cortex reveals compensatory reabsorption capacity of low molecular weight proteins in S3 segment of proximal tubules and collecting ducts  
American Society of Nephrology  
Nov 1 (Oct 30 - Nov 4), 2012 San Diego
  8. Y.Kato, M.Mukoyama, H.Yokoi, Y.Ogawa, K.Mori, M.Kasahara, T.Kuwabara, H.Imamaki, T.Kawanishi, A.Ishii, K.Koga, K.P.Mori, I.Kishimoto, A.Sugawara, K.Nakao  
p38 MAP kinase mediates aldosterone-induced podocyte injury in natriuretic peptide receptor (GC-A)-deficient mice  
American Society of Nephrology

Nov 1 (Oct 30 - Nov 4), 2012 San Diego

9. N.Toda, H.Yokoi, M.Kasahara, K.Mori,  
T.Kuwabara, H.Imamaki, K.Koga, A.Ishii,  
Y.Kato, K.P.Mori, S.Ono, A.Sugawara,  
M.Mukoyama, K.Nakao  
Inducible CTGF (CCN2) Knockout Mice  
Attenuates Anti-Glomerular Basement  
Membrane Nephritis  
American Society of Nephrology  
Nov 1 (Oct 30 - Nov 4), 2012 San Diego

H. 知的財産権の出願・登録状況  
なし

**厚生労働科学研究費補助金（創薬基盤推進研究事業）  
分担研究報告書**

新規創薬を目指した生活習慣病・難治性疾患モデル遺伝子変異ラットの開発と解析  
－糖尿病・メタボリックシンドロームモデル遺伝子変異ラット糖代謝・膵内分泌機能解析－  
分担研究者：富田 努 京都大学大学院医学研究科 内分泌代謝内科 医員

**研究要旨** 本研究課題は、新規開発した標的遺伝子変異ラット開発システムを用いて、生活習慣病や難治性疾患に関連する複数の遺伝子変異ラットを開発し、新規生活習慣病・難治性疾患モデルラットを樹立し、従来マウスにおいて実施・解析が困難であった系統的な生理学的解析、移植実験、薬理薬効評価解析などの施行を容易にする事により、生活習慣病関連疾患、難治性疾患の病態解明、新規治療標的の同定および創薬開発を加速させることを目的とする。本年度は、糖尿病、メタボリックシンドロームに関連した生活習慣病・難治性疾患関連遺伝子変異ラットのスクリーニングの過程で同定し系統樹立した、レプチンおよび Seipin 遺伝子変異ラットの系統樹立の糖代謝、膵内分泌機能に関する解析を行い、興味深い結果を得た。今後も、樹立した遺伝子変異ラットの表現系解析を行い、病態解明研究を行うとともに、新規創薬開発の加速に利用する予定である。

**A. 研究目的**

現在生活習慣病関連疾患である心筋梗塞、心不全、糖尿病、脳卒中、慢性腎臓病(CKD)などの病態解明、新規治療標的の同定に基づく新規治療薬、治療法開発が望まれている。現在これら疾患の病態解析、創薬開発、再生医療研究には遺伝子改変技術が確立されているマウスがモデル動物として多く用いられているが、マウスはその小ささゆえに採血や組織採取(膵臓、中枢神経系)が困難であること、生理学的解析や移植実験が行ないにくいなどの問題がある。さらに、最近では代謝面においてヒトと大きく異なる生理的特徴が明らかとなった(Vassilopoulos, et al. Science 2009)。そのため、マウスと比べ体のサイズが大きく、採血や組織採取や系統的な生理学的解析が容易で、移植実験も行ないやすく、代謝面でもよりヒトに近いラットでの疾患モデル確立が期待されている。しかし、現時点ではES細胞の技術がラットで未確立のため、遺伝子改変ラットの効率的な作成は不可能である。最近京都大学 動物実験施設の芹川、真下らはENU ミュータジェネシスに、新規 DNA スクリーニング法(MuT-power)、凍結精子アーカイブからの個体復元技術(ICSI)という一連の新規技術を組み合わせることにより、標的遺伝子変異ラットの効率的な作成システム構築に成功した。本研究課題では、このシステムを用いて生活習慣病関連・難治性疾患遺伝子変異

ラットをスクリーニングし、その表現系を解析することにより糖尿病、メタボリックシンドロームなどの新規生活習慣病モデルラットを開発し、その詳細な解析を通して病態解明、新規治療標的の同定を行なうと共に、このモデルを用いた新規創薬開発を加速させることを目的とする。

**B. 研究方法**

生活習慣病・難治性疾患関連遺伝子に関するENUミュータジェネシスによる約1600匹分のラットミュータントアーカイブの高速DNAスクリーニングを行い、糖尿病、メタボリックシンドローム関連遺伝子変異として、レプチンおよびseipin遺伝子の変異ラットの同定を行い、その系統樹立に成功した。本年度は特にこれら変異ラットの糖代謝、膵内分泌機能に関して解析をおこなった。これら実験動物を用いる研究に際しては「動物の愛護および管理に関する法律」(平成17年6月改正法)、「京都大学における動物実験の実施に関する規程」および「京都大学大学院医学研究科・医学部における動物実験の実施に関する規程」(いずれも平成19年4月改訂)を遵守して実施し、動物に与える苦痛を最小限にとどめるように最善の配慮を尽くしている。

## C. 研究結果

生活習慣病・難治性疾患関連遺伝子に関するENUミュータジェネシスによる約1600匹分のラットミュータントアーカイブの高速DNAスクリーニングの結果レプチンおよびseipin、遺伝子に変異を有するラットの同定に成功し、さらに独自開発した個体復元技術ICSIを用いて標的遺伝子変異ラット系統樹立に成功し、表現系解析を行った。その結果、レプチン遺伝子ナンセンス変異ラットでは明らかな肥満、耐糖能異常、脂質異常が見出された。また、レプチン遺伝子ナンセンス変異ラットの膵臓では、ラ氏島の拡大を認め、beta細胞などの肥大が考えられた。また、インスリン抵抗性を認めた。一方、脂肪萎縮症の原因遺伝子であるseipin遺伝子の変異ラットの解析も行った。seipin遺伝子変異ラットでは脂肪の減少とインスリン抵抗性が認められ、ヒト脂肪萎縮症と類似の表現系が得られたと考えており、更に詳細な解析を継続している。加えて、seipin遺伝子変異ラットの膵臓の解析を行い、beta細胞面積の増大を認めている。今後さらなる組織学的解析を加える予定である。

## D. 考察

生活習慣病関連疾患の病態解明においては複数の臓器における病態の同時進行的変化とそれに伴う液性因子を介した臓器間シグナルクロストーク解明が必須であり、またこれら病態には細胞老化も関与するため、その治療において細胞・臓器再生という観点も不可欠である。現在これら疾患の病態解析、創薬開発、再生医療研究には遺伝子改変技術が確立されているマウスがモデル動物として多く用いられているが、マウスはその小ささゆえに採血や組織採取が困難であること、生理学的解析や移植実験が行ないにくいなどの問題がある。そのため、マウスと比べ体のサイズが大きく、採血や組織採取や系統的な生理学的解析が容易で、移植実験も行ないやすく、代謝面でもよりヒトに近いラットでの疾患モデル確立が期待されている。実際今回得られたレプチンおよび seipin 遺伝子変異ラットにおいて膵組織の詳細な組織学的解析が可能であることが確認された。今後その表現系を、さらに詳

細に解析することにより、これら遺伝子変異ラットのモデル動物としての意義が確立されれば、病態解明・新規治療標的の同定および新規創薬開発の加速に寄与するものと考えている。

## E. 結論

生活習慣病・難治性疾患関連遺伝子に関して、複数の糖尿病、メタボリックシンドローム関連遺伝子変異ラットの同定、系統樹立に成功し、本年度はその中でレプチンおよび seipin 遺伝子変異ラットの表現系の解析を行った。今後もスクリーニングを継続しつつ、これら遺伝子変異ラットの表現系解析をさらに継続し、疾患モデルラットとしての意義を確立し、病態解明・新規治療標的の同定と新規創薬開発を加速させる予定である。

## F. 健康危険情報

なし

## G. 研究発表

### 1. 論文発表

1. M. Zhao, Y. Li, J. Wang, K. Ebihara, X. Rong, K. Hosoda, T. Tomita, K. Nakao. Azilsartan treatment improves insulin sensitivity in obese spontaneously hypertensive Koletsky rats. *Diabetes Obes Metab.* 13(12) 1123-1129. 2011.

### 2. 学会発表

#### 国際学会

1. T. Tomita, K. Hosoda, S. Odori, Y. Kira, C. Son, J. Fujikura, H. Iwakura, M. Noguchi, E. Mori, M. Naito, T. Kusakabe, K. Ebihara, K. Nakao  
Gene Expression of a G Protein-coupled Receptor, GPR40, in Pancreatic Islets of a Genetically Obese Rat Model  
Keystone Symposia (Killarney, Co. Kerry, Ireland) May 15-20, 2011

#### 国内学会

1. 富田努, 細田公則, 小鳥真司, 藤倉純二, 岩倉浩, 野口倫生, 森栄作, 内藤雅喜, 日下部徹, 海老原健, 中尾一和  
新規のインスリン分泌調節因子 GPR40 の

遺伝子肥満モデルでの発現調節

第 84 回日本内分泌学会学術総会、  
2011. 4. 21-23、神戸

2. 野村英生, 孫徹, 後藤伸子, 勝浦五郎, 野口倫生, 冨田努, 藤倉純二, 海老原健, 細田公則, 中尾一和  
高脂肪食負荷マウス中枢におけるレプチン反応性の経時的変化の検討  
第 84 回日本内分泌学会学術総会、  
2011. 4. 21-23、神戸
3. 小鳥真司, 冨田努, 孫徹, 藤倉純二, 野口倫生, 森栄作, 内藤雅喜, 日下部徹, 海老原健, 細田公則, 中尾一和  
新規の G 蛋白共役型・脂質受容体 GPR119 の臨床的意義: ヒトおよびマウスでの膵島における遺伝子発現と膵島機能との連関  
第 84 回日本内分泌学会学術総会、  
2011. 4. 21-23、神戸
4. 阿部恵, 海老原健, 海老原千尋, 宮澤崇, 冨田努, 日下部徹, 山本祐二, 宮本理人, 真下知士, 細田公則, 芹川忠夫, 中尾一和  
糖脂質代謝におけるレプチンの病態生理的意義に関する種族差の検討ーレプチン欠損 ob/ob ラットの開発と解析ー  
第 84 回日本内分泌学会学術総会  
2011. 4. 21-23、神戸
5. 内藤雅喜, 藤倉純二, 森栄作, 小鳥真司, 野口倫生, 冨田努, 孫徹, 日下部徹, 宮永史子, 宮本理人, 山本祐二, 海老原健, 細田公則, 中尾一和  
Leptin Transgenic Akita mouse を用いたインスリン分泌低下型糖尿病に対するレプチン治療  
第 84 回日本内分泌学会学術総会  
2011. 4. 21-23、神戸
6. 井田みどり, 榊田出, 細田公則, 海老原健, 藤倉純二, 岩倉浩, 日下部徹, 山本祐二, 阿部恵, 冨田努, 葛谷英嗣, 中尾一和  
Dual Bioimpedance 法を用いた内臓脂肪量測定装置のスクリーニング機器としての有用性  
第 84 回日本内分泌学会学術総会  
2011. 4. 21-23、神戸
7. 冨田努, 細田公則, 小鳥真司, 孫徹, 藤倉純二, 岩倉浩, 野口倫生, 森栄作, 内藤雅喜, 吉良友里, 日下部徹, 海老原健, 益崎裕章, 中尾一和  
膵β細胞に高発現し、中・長鎖脂肪酸をリガンドする G 蛋白共役型受容体 GPR40 の遺伝性肥満モデルの膵島での発現調節  
第 54 回日本糖尿病学会年次学術集会、  
2011. 5. 19-21、札幌
8. 阿部恵, 海老原健, 海老原千尋, 宮澤崇, 冨田努, 日下部徹, 山本祐二, 宮本理人, 真下知士, 細田公則, 芹川忠夫, 中尾一和  
レプチン欠損 ob/ob ラットの開発と糖脂質代謝解析  
第 54 回日本糖尿病学会年次学術集会、  
2011. 5. 19-21、札幌
9. 内藤雅喜, 藤倉純二, 森栄作, 小鳥真司, 野口倫生, 冨田努, 孫徹, 日下部徹, 宮永史子, 宮本理人, 山本祐二, 海老原健, 細田公則, 中尾一和  
Leptin Transgenic Akita マウスを用いたインスリン分泌低下型糖尿病に対するレプチン治療  
第 54 回日本糖尿病学会年次学術集会、  
2011. 5. 19-21、札幌
10. 細田公則, 井田みどり, 榊田出, 海老原健, 藤倉純二, 岩倉浩, 日下部徹, 山本祐二, 阿部恵, 冨田努, 葛谷英嗣, 中尾一和  
Dual Bioimpedance 法を用いた内臓脂肪量測定装置のスクリーニング機器としての有用性  
第 54 回日本糖尿病学会年次学術集会、  
2011. 5. 19-21、札幌
11. 野村英生, 孫徹, 野口倫生, 冨田努, 藤倉純二, 海老原健, 細田公則, 中尾一和  
高脂肪食負荷レプチン抵抗モデルマウスにおける部位特異的レプチン反応性の検討  
第 54 回日本糖尿病学会年次学術集会、  
2011. 5. 19-21、札幌

12. 小島真司, 冨田努, 孫徹, 藤倉純二, 野口倫生, 森栄作, 内藤雅喜, 日下部徹, 海老原健, 細田公則, 中尾一和  
新規の G 蛋白共役型・脂質受容体 GPR119 の臨床的意義：ヒトおよびマウスでの膵島における遺伝子発現と膵島機能との関連  
第 54 回日本糖尿病学会年次学術集会、  
2011. 5. 19-21、札幌
13. 冨田努, 細田公則, 小島真司, 孫徹, 藤倉純二, 岩倉浩, 野口倫生, 日下部徹, 海老原健, 中尾一和  
G 蛋白共役型・脂肪酸受容体 GPR40 の遺伝性肥満モデルの膵島での発現調節  
第 32 回日本肥満学会 学術集会、  
2011.9.23-24、兵庫県淡路島
14. 孫徹, 野村英生, 後藤伸子, 勝浦五郎, 野口倫生, 冨田努, 藤倉純二, 海老原健, 細田公則, 中尾一和  
高脂肪食負荷レプチントランスジェニックマウス中枢におけるレプチン反応性の検討  
第 32 回日本肥満学会 学術集会、  
2011.9.23-24、兵庫県淡路島
15. 内藤雅喜, 藤倉純二, 森栄作, 野口倫生, 冨田努, 孫徹, 日下部徹, 海老原健, 細田公則, 中尾一和  
Leptin Transgenic Akita mouse を用いたインスリン分泌低下型糖尿病に対するレプチン治療  
第 32 回日本肥満学会 学術集会、  
2011.9.23-24、兵庫県淡路島
16. 小島真司, 冨田努, 孫徹, 藤倉純二, 野口倫生, 森栄作, 内藤雅喜, 日下部徹, 海老原健, 細田公則, 中尾一和  
G 蛋白共役型・脂肪酸受容体 GPR40 の遺伝性肥満モデルの膵島での発現調節  
第 32 回日本肥満学会 学術集会、  
2011.9.23-24、兵庫県淡路島

H. 知的財産権の出願・登録状況  
なし



研究成果の刊行に関する一覧表

雑誌

発表者氏名	論文タイトル名	発表誌名	巻号	ページ	出版年
Yokoi, H., Kasahara, M., Mori, K., Kuwabara, T., Toda, N., Yamada, R., Namoto, S., Yamamoto, T., Seki, N., So uma, N., Yamaguchi, T., Sugawara, A., Mukoyama, M., and Nakao, K.	Peritoneal fibrosis and high transpoare induced in mildly pre-injured peritoneum by 3,4-dideoxyglucosone-3-ene in mice.	Perit. Dial. Int.	33	143-154	2013
Ogawa, Y., Mukoyama, M., Yokoi, H., Kasahara, M., Mori, K., Kato, Y., Kuwabara, T., Imamaki, H., Kawanishi, T., Koga, K., Ishii, A., Tokudome, T., Kishimoto, I., Sugawara, A., Nakao, K.	Natriuretic peptide receptor guanylyl cyclase-A protects podocytes from aldosterone-induced glomerular injury.	J. Am. Soc. Nephrol.	23	1198-1209	2012
Yokoi, H., Kasahara, M., Mori, K., Ogawa, Y., Kuwabara, T., Imamaki, H., Kawanishi, T., Koga, K., Ishii, A., Kato, Y., Mori, P. K., Toda, N., Ohno, S., Muramatsu, H., Muramatsu, T., Sugawara, A., Mukoyama, M., and Nakao, K.	Pleiotrophin triggers inflammation and increased peritoneal permeability leading to peritoneal fibrosis.	Kidney Int.	81	160-169	2012
Kuwabara, T., Mori, K., Mukoyama, M., Kasahara, M., Yokoi, H., Saito, Y., Ogawa, Y., Imamaki, H., Kawanishi, T., Ishii, A., Koga, K., Mori, PK., Kato, Y., Sugawara, A., Nakao, K.	Exacerbation of diabetic nephropathy by hyperlipidaemia is mediated by toll-like receptor 4 in mice.	Diabetologia	81	160-169	2012
N. Yamada-Goto, G. Katsuura, K. Ebihara, M. Inuzuka, Y. Ochi, Y. Yamashita, T. Kusakabe, A. Yasoda, N. Asahara- Satoh, H. Ariyasu, K. Hosoda, K. Nakao.	Intracerebroventricular administration of C-type natriuretic peptide suppresses food intake via activation of the melanocortin system in mice.	Diabetes..		In press	2012
L. Miyamoto, K. Ebihara, T. Kusakabe, D. Aotani, S. Yamamoto-Kataoka, T. Sakai, M. Aizawa-Abe, Y. Yamamoto, J. Fujikura, T. Hayashi, K. Hosoda, K. Nakao.	Leptin activates hepatic 5' AMP-Activated Protein Kinase through sympathetic nervous system and $\alpha 1$ adrenergic receptor: A potential mechanism for improvement of fatty liver in lipodystrophy by leptin.	J Biol Chem.	287	40441-40447	2012
M. Iwanishi, K. Ebihara, T. Kusakabe, S. Harada, J. Ito-Kobayashi, A. Tsuji, K. Hosoda, K. Nakao K.	Premature atherosclerosis in a Japanese diabetic patient with atypical familial partial lipodystrophy and hypertriglyceridemia.	Intern Med.	51	2573-2579,	2012

D. Aotani, K. Ebihara, N. Sawamoto, T. Kusakabe, M. Aizawa-Abe, S. Kataoka, T. Sakai, H. Iogawa, C. Ebihara, J. Fujikura, K. Hosoda, H. Fukuyama, K. Nakao.	Functional Magnetic Resonance Imaging Analysis of Food-Related Brain Activity in Patients with Lipodystrophy Undergoing Leptin Replacement Therapy.	J Clin Endocrinol Metab.	97	3663- 3671	2012
N. Yamada-Goto, G. Katsuura, Y. Ochi, K. Ebihara, T. Kusakabe, K. Hosoda, K. Nakao.	Impairment of fear-conditioning responses and changes of brain neurotrophic factors in diet-induced obese mice.	J Neuroendocrinol.	24	1120-1125	2012
T. Kusakabe, K. Ebihara, T. Sakai, L. Miyamoto, D. Aotani, Y. Yamamoto, S. Yamamoto-Kataoka, M. Aizawa-Abe, J. Fujikura, K. Hosoda, K. Nakao.	Amylin improves the effect of leptin on insulin sensitivity in leptin-resistant diet-induced obese mice.	Am J Physiol Endocrinol Metab.	302	E924-931	2012
Nishikimi T, Okamoto H, Nakamura M, Ogawa N, Horii K, Nagata K, Nakagawa Y, Kinoshita H, Yamada C, Nakao K, Minami T, Kuwabara Y, Kuwahara K, Masuda I, Kangawa K, Minamino N, Nakao K.	Direct immunochemiluminescent assay for proBNP and total BNP in human plasma proBNP and total BNP levels in normal and heart failure	PLoS One.	8	e53233	2013
Nishikimi T, Kuwahara K, Nakagawa Y, Kangawa K, Minamino N, Nakao K.	Complexity of meliclar forms of B-type natriuretic peptide in heart failure.	Heart		In press	2012
Minami T, Kuwahara K, Nakagawa Y, Takaoka M, Kinoshita H, Nakao K, Kuwabara Y, Yamada Y, Yamada C, Shibata J, Usami S, Yasuno S, Nishikimi T, Ueshima K, Sata M, Nakano H, Seno T, Kawahito Y, Sobue K, Kimura A, Nagai R, Nakao K.	Reciprocal expression of MRTF-A and myocardin is crucial for pathological vascular remodelling in mice.	EMBO J	31	4428-40	2012

## PERITONEAL FIBROSIS AND HIGH TRANSPORT ARE INDUCED IN MILDLY PRE-INJURED PERITONEUM BY 3,4-DIDEOXYGLUCOSONE-3-ENE IN MICE

Hideki Yokoi,<sup>1</sup> Masato Kasahara,<sup>1</sup> Kiyoshi Mori,<sup>1</sup> Takashige Kuwabara,<sup>1</sup> Naohiro Toda,<sup>1</sup> Ryo Yamada,<sup>2</sup> Shinji Namoto,<sup>2</sup> Takashi Yamamoto,<sup>2</sup> Nana Seki,<sup>2</sup> Nozomi Souma,<sup>2</sup> Taku Yamaguchi,<sup>2</sup> Akira Sugawara,<sup>1</sup> Masashi Mukoyama,<sup>1</sup> and Kazuwa Nakao<sup>1</sup>

Department of Medicine and Clinical Science,<sup>1</sup> Kyoto University Graduate School of Medicine, Kyoto, and Research and Development,<sup>2</sup> JMS Co. Ltd., Hiroshima, Japan

Peritoneal dialysis (PD) solution contains high concentrations of glucose and glucose degradation products (GDPs). One of several GDPs—3,4-dideoxyglucosone-3-ene (3,4-DGE)—was recently identified as the most reactive and toxic GDP in PD fluids. *In vitro*, 3,4-DGE has been shown to induce mesothelial cell damage; however, its role in peritoneal fibrosis *in vivo* remains unclear. In the present study, we intraperitoneally administered chlorhexidine gluconate (CG) for mild peritoneal injury, and we then injected 3,4-DGE [38  $\mu$ mol/L (low concentration) or 145  $\mu$ mol/L (high concentration)] 5 times weekly for 4 weeks. Significant thickening of the parietal peritoneal membrane was observed only when treatment with low or high concentrations of 3,4-DGE occurred after CG administration, but not when either CG or 3,4-DGE alone was given. The combination of CG and 3,4-DGE also caused upregulation of messenger RNA expression of transforming growth factor  $\beta$ 1, connective tissue growth factor, fibronectin, collagen type 1  $\alpha$ 1 chain, alpha smooth muscle actin ( $\alpha$ -SMA), vascular endothelial growth factor 164, NADPH oxidase 1 and 4, p22phox, p47phox, and gp91phox in peritoneal tissue. Treatment with CG alone was sufficient to cause significant F4/80-positive macrophage infiltration, appearance of  $\alpha$ -SMA-positive cells, and vessel formation in the submesothelial layer. Addition of 3,4-DGE markedly enhanced those changes and induced apoptosis, mainly in leukocytes. The concentration of 3,4-DGE in the abdominal cavity declined more rapidly in CG-treated mice than in PBS-treated mice. Peritoneal membrane permeability determined by peritoneal equilibration test showed high transport conditions in peritoneum treated with both CG and 3,4-DGE. These results indicate that, when mild peritoneal damage is already present, 3,4-DGE causes peritoneal thickening and fibrosis, resulting in deterioration of peritoneal membrane function.

Correspondence to: M. Kasahara, Department of Medicine and Clinical Science, Kyoto University Graduate School of Medicine, 54 Shogoin Kawahara-cho, Sakyo-ku, Kyoto 606-8507 Japan.

kasa@kuhp.kyoto-u.ac.jp

Received 9 February 2011; accepted 9 April 2012

Perit Dial Int 2013; 33(2):143–154 www.PDIConnect.com  
epub ahead of print: 01 Nov 2012 doi:10.3747/pdi.2011.00033

KEY WORDS: Peritoneum; mesothelial cells; 3,4-DGE; apoptosis; macrophages; angiogenesis; chlorhexidine gluconate.

Peritoneal dialysis (PD) is a well-established method of home dialysis for patients with end-stage renal failure. During long-term PD, the peritoneal membrane develops peritoneal fibrosis in response to a variety of injuries, including bioincompatible PD solutions, peritonitis, uremia, and chronic inflammation (1,2). Solutions for PD contain high concentrations of glucose, which result in glucose degradation products (GDPs) during the process of heat sterilization. Some GDPs identified in PD fluid (3,4) include acetaldehyde, 3-deoxyglucosone, formaldehyde, 2-furaldehyde, glyoxal, 5-hydroxymethylfurfural, methylglyoxal (MGO), and 3,4-dideoxyglucosone-3-ene (3,4-DGE). Among those GDPs, the highly reactive 3,4-DGE is a toxic substance in PD fluid (4,5). Recently, PD fluid with a neutral pH and lower GDPs has shown improved performance, as indicated by reduced levels of inflammatory markers in effluent and of circulating advanced glycation endproducts (6).

Fluids containing high GDP levels are relevant to peritoneal fibrosis and loss of ultrafiltration (7,8). Although the mechanisms of GDP cytotoxicity are not fully understood, 3,4-DGE has been shown to affect the cytotoxicity of acidic, heat-sterilized PD fluid on human peritoneal mesothelial cells (9). In particular, 3,4-DGE induces apoptosis and epithelial–mesenchymal transition (EMT) in peritoneal mesothelial cells (10). The concentration of 3,4-DGE in conventional PD fluids is normally 10–38  $\mu$ mol/L (4,5), enough to promote mesothelial cell apoptosis (10). The high reactivity of

3,4-DGE is responsible for depletion of total intracellular glutathione (9), suggesting that 3,4-DGE can enhance oxidative stress in peritoneal mesothelial cells (11). Infusion of conventional PD solution containing an intermediate level of GDPs and lipopolysaccharide (compared with low-GDP solution and lipopolysaccharide) induced high peritoneal transport in rats (12,13). Low-GDP solution caused less peritoneal injury and submesothelial vascularization in rats (14).

Peritoneal dialysis fluid containing GDPs is closely associated with EMT of peritoneal mesothelial cells *in vivo* (15). However, it is not clear whether 3,4-DGE plays a role in peritoneal damage *in vivo*, because no report has shown that 3,4-DGE induces peritoneal fibrosis in that situation. We therefore used two doses of 3,4-DGE—38  $\mu\text{mol/L}$ , the highest found in conventional PD fluid, and 145  $\mu\text{mol/L}$ , higher than the amount found in PD fluid—to examine the role of 3,4-DGE in peritoneal fibrosis and inflammation *in vivo*. We also examined whether pre-existing chlorhexidine gluconate (CG)—induced peritoneal injury increases 3,4-DGE-induced peritoneal injury.

## METHODS

### ANIMAL MODELS

All animal experiments were approved by the animal experimentation committee of Kyoto University Graduate School of Medicine. Purification of 3,4-DGE was performed as previously described (11). We treated C57BL/6J mice weighing approximately 26 g with intraperitoneal injections of 0.3 mL 0.1% CG in 15% ethanol and 85% phosphate-buffered saline (PBS) every other day for 1 week; they were then injected with 38  $\mu\text{mol/L}$  or 145  $\mu\text{mol/L}$  3,4-DGE dissolved in 1 mL PBS every weekday for 4 weeks without antibiotics. Control mice received PBS only. Mice were assigned randomly to one of the following groups:

- Group 1: initial PBS and subsequent PBS without 3,4-DGE [PBS+3,4-DGE(-)],  $n = 10$
- Group 2: initial PBS and subsequent 38  $\mu\text{mol/L}$  3,4-DGE (PBS+38  $\mu\text{mol/L}$  3,4-DGE),  $n = 8$
- Group 3: initial PBS and subsequent 145  $\mu\text{mol/L}$  3,4-DGE (PBS+145  $\mu\text{mol/L}$  3,4-DGE),  $n = 5$
- Group 4: initial CG and subsequent PBS without 3,4-DGE [CG+3,4-DGE(-)],  $n = 8$
- Group 5: initial CG and subsequent 38  $\mu\text{mol/L}$  3,4-DGE (CG+38  $\mu\text{mol/L}$  3,4-DGE),  $n = 11$
- Group 6: initial CG and subsequent 145  $\mu\text{mol/L}$  3,4-DGE (CG+145  $\mu\text{mol/L}$  3,4-DGE),  $n = 5$

### QUANTITATIVE ANALYSIS OF 3,4-DGE IN PLASMA AND PERITONEAL EFFLUENT

The concentration of 3,4-DGE in the abdominal cavity was evaluated. Mice were injected with PBS ( $n = 8$ ) or 0.1% CG ( $n = 7$ ) every other day for 1 week. Then, using an 18G needle, 4 mL 3,4-DGE diluted in PBS was injected into the peritoneal cavity of the mice. Peritoneal solution was collected at 1, 10, 20, and 30 minutes after injection. At 30 minutes after injection, blood samples were collected using heparin-coated capillary tubes from mice given 145  $\mu\text{mol/L}$  3,4-DGE ( $n = 2$  from the PBS group,  $n = 3$  from the CG group). Blood samples were centrifuged and plasma components were separated.

The concentrations of 3,4-DGE in plasma and peritoneal effluent were analyzed by liquid chromatography–mass spectrometry as a quinoxaline derivative after a reaction with 2,3-diamino naphthalene. Briefly, 50  $\mu\text{L}$  of sample or standard solution was diluted with an equivalent amount of 0.2 mol/L sodium phosphate buffer (pH 7.4). Then 100  $\mu\text{L}$  of 0.05% 2,3-diamino naphthalene (Tokyo Chemical Industry, Tokyo, Japan) in acetonitrile was added to the solution and carefully mixed. For deproteinization, the mixture was centrifuged (6000g for 10 minutes), after which an aliquot of the supernatant was incubated at 25°C for 20 hours under dark conditions for derivative formation. The reaction solution was assayed by reverse-phase high-performance liquid chromatography using a Symmetry column (Waters, Milford, MA, USA) with 25% – 65% gradient elution of acetonitrile containing 0.1% formic acid. The 3,4-DGE-quinoxaline derivative was then detected as protonated molecular ion at 267.1 Da [ $\text{C}_{16}\text{H}_{14}\text{N}_2\text{O}_2 + \text{H}$ ]<sup>+</sup> by electrospray positive-ionization mass spectrometry.

The preliminary experiment confirmed that the blood component inhibited the reaction between 3,4-DGE and 2,3-diaminonaphthalene, and therefore, to minimize the inhibitory effect, the calibration standards were prepared using serum. For analysis of the peritoneal fluid, aqueous solutions of 3,4-DGE were used as calibration standards. All standard solutions were treated using identical derivatization processing.

### MODIFIED PERITONEAL EQUILIBRATION TEST

Before the mice were humanely euthanized, a modified peritoneal equilibration test was performed to determine peritoneal permeability as previously described (16). Briefly, the mice (group 1:  $n = 3$ ; group 2:  $n = 3$ ; group 4:  $n = 3$ ; group 5:  $n = 5$ ) were given 3-mL intraperitoneal injections of 7% glucose dialysis solution (Perisate: JMS, Hiroshima, Japan). After a 2-hour dwell, effluents

were collected and blood samples were drawn. Serum and dialysate creatinine and urea nitrogen levels were measured by the enzymatic method (SRL, Tokyo, Japan). Calculation of the mass transfer-area coefficient (MTAC) of urea was calculated as previously described (17). Mice were euthanized under anesthesia at 5 weeks after CG-treatment, and samples were collected for histologic and biochemical analyses.

### HISTOLOGY AND IMMUNOHISTOCHEMICAL STUDY FOR THE PERITONEUM

Anterior abdominal walls containing parietal peritoneum were fixed with 4% buffered paraformaldehyde and embedded in paraffin. We measured the thickness of the fibrotic submesothelial zone above the abdominal muscle layer in cross-sections as previously described (18).

For immunohistochemical analyses of F4/80, CD31, and cytokeratin, the sections were processed as described, with some modifications (18,19). After 0.1% trypsin-mediated antigen retrieval, the samples were incubated with rat monoclonal anti-F4/80 antibody (Serotec, Oxford, UK), rat monoclonal anti-CD31 antibody (BD Biosciences, San Diego, CA, USA), or rabbit polyclonal anti-cytokeratin antibody (Dako, Glostrup, Denmark). After incubation with biotin-conjugated secondary anti-rat immunoglobulin G antibody (Vector Laboratories, Burlingame, CA, USA), the specimens were treated with streptavidin-conjugated horseradish peroxidase (Dako) and then developed using 3,3'-diaminobenzidine tetrahydrochloride (Dako). For immunohistochemical analyses of alpha smooth muscle actin ( $\alpha$ -SMA), the sections were processed using microwave-mediated antigen retrieval and were then incubated with rabbit polyclonal anti- $\alpha$ -SMA antibody (Abcam, Cambridge, UK).

### REAL-TIME POLYMERASE CHAIN REACTION ANALYSIS

Quantitative real-time polymerase chain reaction was performed using Premix Ex Taq (Takara Bio, Shiga, Japan) on an Applied Biosystems 7300 real-time polymerase chain reaction system (Applied Biosystems, Foster City, CA, USA) or a StepOnePlus system (Applied Biosystems) as previously described, with some modifications (18,19). Gene-specific primers and probes were then used to determine the expression levels of mouse transforming growth factor  $\beta$ 1 (TGF- $\beta$ 1), connective tissue growth factor (CTGF), fibronectin, collagen type 1 alpha 1 chain (COL1A1),  $\alpha$ -SMA, vascular endothelial growth factor 164 (VEGF164), NADPH oxidase 1 (NOX1) and 4 (NOX4), p22phox, p47phox, and gp91phox (Table 1). Expression

TABLE 1  
TaqMan primers and probe sequences<sup>a</sup>

Gene	Forward primer	Reverse primer	Probe
TGF- $\beta$ 1	5'-GACGTCACGTGGAGTTGTACGG-3'	5'-GCTGAATCGAAAGCCCTGT-3'	5'-FAM-AGTGGCTGAACCAAGGAGACGGAA-TAMRA-3'
CTGF	5'-JTCCCGAGAAGGGTCAAGCT-3'	5'-TCTTGGGCTCGTCACACA-3'	5'-FAM-CCTGGAAATGCTCAAGGAGTGG-TAMRA-3'
Fibronectin	5'-ATCAATTCATGCAACAGTT-3'	5'-TGCACCTGGTAGAAGTTCCA-3'	5'-FAM-CCGAGGAAGAGCCCTACAGTTCCA-TAMRA-3'
COL1A1	5'-GTCCCAACCCCAAGAC-3'	5'-CACTCTGAGTTTGGTGATAGT-3'	5'-FAM-TGCTGTGCTTCTGCCCGGA-TAMRA-3'
$\alpha$ -SMA	5'-CCTGACGCTGAAGTATCCGATAG-3'	5'-GGTGCCAGATCTTTTCCATGTC-3'	5'-FAM-ACACGGCATCATCAACTCTGGGA-TAMRA-3'
VEGF164	5'-AACGATGAAGCCCTGGAGT-3'	5'-GACAAACAATGCTTTCTCCG-3'	5'-FAM-CTGTAGGAAGCTCTCTCTCTATGTC-TAMRA-3'
NOX1	5'-TCGTCTATATCATCTGCTTAGGGATC-3'	5'-GGCTTTTCCCAAGCTCTCC-3'	5'-FAM-GGCTTTTCCCAAGCTCTCC-TAMRA-3'
NOX4	5'-GCAAGACTCTACACATCATGTG-3'	5'-TGCTGATTCAGTTCAGGAAATC-3'	5'-FAM-TCTCAGGTGTGATGATAGCCGCCCA-TAMRA-3'
p22phox	5'-CCCTCACCAGGAATTACTACG-3'	5'-CACTGCTCACCTCGGATGG-3'	5'-FAM-CTCCACTTCTGTGCTGGTGCCTGC-TAMRA-3'
p47phox	5'-GGCGAGATCCACAGAGAAC-3'	5'-CGTTGAAGTATTCAGTGAGATGTC-3'	5'-FAM-TCCCACACTCCCGGACCCAG-TAMRA-3'
gp91phox	5'-GGTGACAATGAGAACGAGATATC-3'	5'-GAGACACAGTGTGATGACAATTCC-3'	5'-FAM-CAGCCAACCGAGTACGCGCCACATAC-TAMRA-3'

TGF- $\beta$ 1 = transforming growth factor  $\beta$ 1; CTGF = connective tissue growth factor; COL1A1 = collagen type 1  $\alpha$ 1 chain;  $\alpha$ -SMA = alpha smooth muscle actin, VEGF = vascular endothelial growth factor; NOX = NADPH oxidase; p22phox = cytochrome b-245, alpha polypeptide; p47phox = neutrophil cytosolic factor 1; gp91phox = cytochrome b245, beta polypeptide.

<sup>a</sup> Purchased from Applied Biosystems and Sigma Genosys, Tokyo, Japan.

of each messenger RNA (mRNA) was normalized to GAPDH mRNA (TaqMan rodent GAPDH control reagents: Applied Biosystems).

# ASSESSMENT OF APOPTOSIS

Apoptosis was quantified using a terminal deoxynucleotidyl transferase-mediated dUTP nick end labeling (TUNEL) assay with *in situ* cell death detection kit and fluorescein (Roche, Basel, Switzerland) as previously described (20). To detect apoptotic cell types, triple staining for CD45, TUNEL, and DAPI was performed. Paraffin-embedded peritoneal sections 4  $\mu$ m in thickness were deparaffinized and treated with microwaves for antigen retrieval. Sections were then processed with rabbit polyclonal anti-CD45 antibody (Abcam) for 1 hour at room temperature. After incubation with DyLight 549 conjugated donkey anti-rabbit antibody (Jackson ImmunoResearch, West Grove, PA, USA), the sections were treated with 0.1% Triton X in 0.1% sodium citrate buffer and then incubated with TUNEL reaction mixture.

# STATISTICAL ANALYSIS

Data are expressed as mean  $\pm$  standard error of the mean. The statistical analysis was performed using one-way analysis of variance or the Student t-test, as appropriate. A *p* value of less than 0.05 was considered statistically significant.

# RESULTS

## PRETREATMENT WITH CG ENHANCES 3,4-DGE-INDUCED PERITONEAL FIBROSIS

Mice received intraperitoneal injections of PBS every other day for 1 week (3 times) and then injections of low (38  $\mu$ mol/L) or high (145  $\mu$ mol/L) concentrations 3,4-DGE every weekday for 4 weeks. Mice treated with 3,4-DGE or CG (or both) and mice receiving PBS+3,4-DGE(-) all had similar body weights (Figure 1). The thickness of the peritoneal membrane was analyzed using Masson trichrome staining. The PBS+3,4-DGE(-) and 38  $\mu$ mol/L or 145  $\mu$ mol/L PBS+3,4-DGE mice showed almost normal peritoneal tissues. Notably, the thickness of the peritoneal membrane was greater for CG+38  $\mu$ mol/L 3,4-DGE mice than for CG+3,4-DGE(-) mice. The CG+145  $\mu$ mol/L 3,4-DGE mice showed even more pronounced peritoneal membrane thickness: PBS+3,4-DGE(-),  $27.9 \pm 4.8$   $\mu$ m; PBS+38  $\mu$ mol/L 3,4-DGE,  $23.5 \pm 1.6$   $\mu$ m; PBS+145  $\mu$ mol/L 3,4-DGE,  $26.8 \pm 4.1$   $\mu$ m; CG+3,4-DGE(-),  $47.2 \pm 1.7$   $\mu$ m;

CG+38  $\mu$ mol/L 3,4-DGE,  $142 \pm 11$   $\mu$ m; CG+145  $\mu$ mol/L 3,4-DGE,  $253 \pm 16$   $\mu$ m (Figure 2).

## EFFECT OF CG AND 3,4-DGE ON GENE EXPRESSION IN PERITONEAL INJURY

We next examined gene expression of TGF- $\beta$ 1, CTGF, fibronectin, COL1A1,  $\alpha$ -SMA, and VEGF164 in peritoneum (Figure 3). Administration of 38  $\mu$ mol/L or 145  $\mu$ mol/L 3,4-DGE in PBS-treated mice did not increase mRNA expression of TGF- $\beta$ 1, CTGF, fibronectin, COL1A1,  $\alpha$ -SMA, and VEGF164. Compared with CG+3,4-DGE(-) mice, the CG+145  $\mu$ mol/L 3,4-DGE mice showed increased TGF- $\beta$ 1, CTGF, fibronectin, COL1A1,  $\alpha$ -SMA, and VEGF164 expression, suggesting that the combination of CG and 3,4-DGE enhances extracellular matrix production.

Next, we examined the expression of NOX1, NOX4, p22phox, p47phox, and gp91phox, which are essential membrane components of NAD(P)H oxidase, in peritoneum. Compared with PBS+3,4-DGE(-) mice, the PBS+38  $\mu$ mol/L 3,4-DGE mice did not show increases in mRNA expression for those components. Compared with PBS+3,4-DGE(-) mice, the PBS+145  $\mu$ mol/L 3,4-DGE

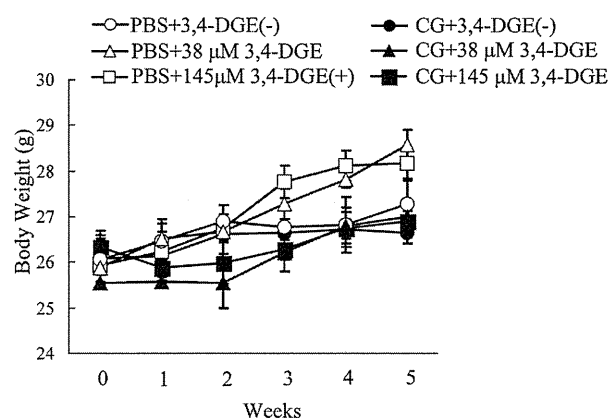


Figure 1 — Time course of body weight in mice. Mice were treated with intraperitoneal injections of 0.1% chlorhexidine gluconate (CG) or phosphate buffered saline (PBS) every other day for a week. They were then injected with 38  $\mu$ mol/L or 145  $\mu$ mol/L 3,4-dideoxyglucosone-3-ene (3,4-DGE) or PBS every weekday for 4 weeks. Initial PBS followed by PBS without 3,4-DGE (*n* = 10, open circles); initial PBS followed by PBS plus 38  $\mu$ mol/L 3,4-DGE (*n* = 8, open triangles); initial PBS followed by PBS with 145  $\mu$ mol/L 3,4-DGE (*n* = 5, open squares); initial CG followed by PBS without 3,4-DGE (*n* = 8, closed circles); initial CG followed by PBS with 38  $\mu$ mol/L 3,4-DGE (*n* = 11, closed triangles); CG plus 145  $\mu$ mol/L followed by PBS with 3,4-DGE (*n* = 5, close squares). All mice were compared with mice receiving PBS without 3,4-DGE; no significant differences were observed.

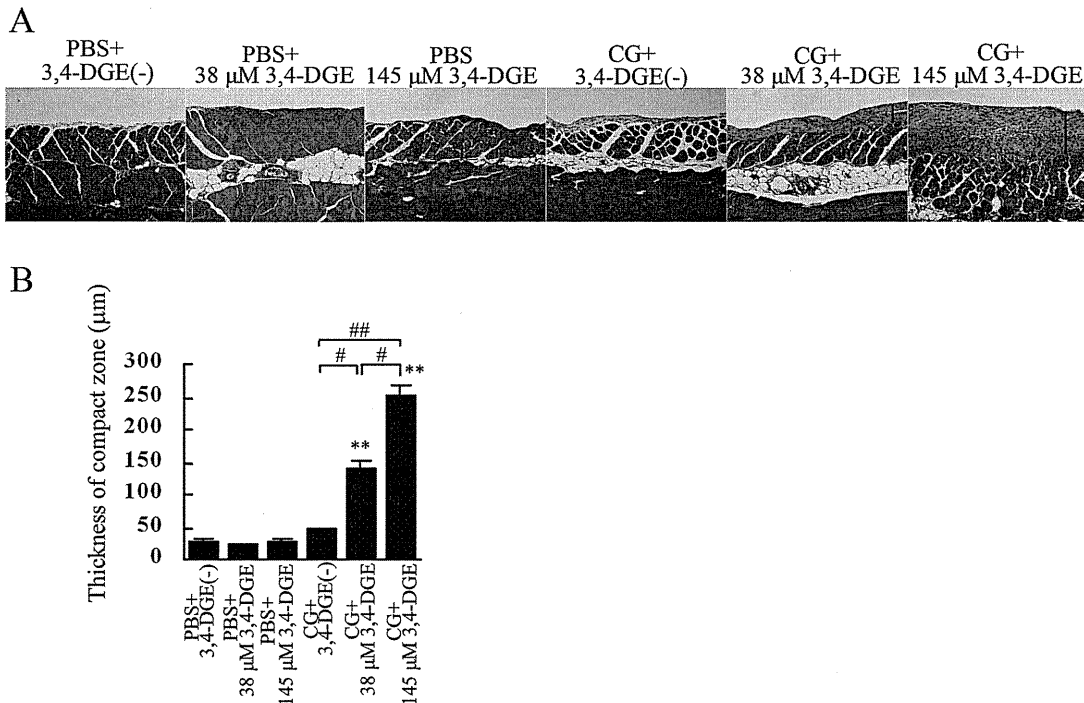


Figure 2 — Histologic appearance of the peritoneum in each group. (A) Compared with mice treated with phosphate-buffered saline (PBS) plus 38  $\mu\text{mol/L}$  3,4-dideoxyglucosone-3-ene (3,4-DGE), mice treated with chlorhexidine gluconate (CG) plus 38  $\mu\text{mol/L}$  3,4-DGE showed thickened peritoneum. In mice treated with CG+145  $\mu\text{mol/L}$  3,4-DGE, peritoneal fibrosis was more pronounced. Arrows indicate the submesothelial compact zone (Masson trichrome stain). (B) Thickness of the peritoneal membrane (mean  $\pm$  standard error of the mean) in mice under various conditions: PBS without 3,4-DGE [PBS+3,4-DGE(-),  $n = 7$ ]; PBS+38  $\mu\text{mol/L}$  3,4-DGE ( $n = 5$ ); PBS+145  $\mu\text{mol/L}$  3,4-DGE ( $n = 5$ ); CG+3,4-DGE(-) ( $n = 5$ ); CG+38  $\mu\text{mol/L}$  3,4-DGE ( $n = 6$ ); CG+145  $\mu\text{mol/L}$  3,4-DGE ( $n = 5$ ). \*\*  $p < 0.01$  versus mice treated with PBS and same dose of 3,4-DGE; #  $p < 0.05$ ; ##  $p < 0.01$ .

mice showed increased mRNA expression of p22phox. The CG+38  $\mu\text{mol/L}$  3,4-DGE mice showed higher expression of NOX1 and NOX4 than did CG+3,4-DGE(-) mice. In CG+145  $\mu\text{mol/L}$  3,4-DGE mice, NOX4, p47phox, and gp91phox mRNA expression were higher than the expression observed in PBS+3,4-DGE(-) mice. These results suggest that the combination of CG and 3,4-DGE can increase oxidative stress.

#### MACROPHAGE RECRUITMENT, $\alpha$ -SMA-POSITIVE CELLS, AND VASCULAR VESSELS

Macrophage infiltration was assessed by immunohistochemistry for F4/80 [Figure 4(A)]. The number of macrophages in peritoneum was very small in PBS+3,4-DGE(-) and 38  $\mu\text{mol/L}$  or 145  $\mu\text{mol/L}$  PBS+3,4-DGE mice [Figure 4(B)]. In CG+3,4-DGE(-) mice, significantly increased numbers of F4/80-positive cells were observed around the submesothelial compact zone. Although the presence of 38  $\mu\text{mol/L}$  3,4-DGE did not change the number of infiltrating macrophages, the numbers of those cells were markedly increased in CG+145  $\mu\text{mol/L}$

3,4-DGE mice compared with CG+3,4-DGE(-) mice ( $85.1 \pm 9.4$  vs  $5.8 \pm 1.1$ ). These results indicate that 3,4-DGE alone did not increase macrophage infiltration at the concentrations tested, but that 3,4-DGE augmented macrophage infiltration in the presence of pre-existing peritoneal injury.

We next examined  $\alpha$ -SMA-positive cells using immunohistochemistry [Figure 4(A)]. The expression of  $\alpha$ -SMA was confined to vascular smooth muscle cells in PBS-treated mice. In CG-treated mice,  $\alpha$ -SMA-positive cells were localized in the submesothelial compact zone. The numbers of  $\alpha$ -SMA-positive cells were significantly higher in both 38  $\mu\text{mol/L}$  and 145  $\mu\text{mol/L}$  CG+3,4-DGE mice than in CG+3,4-DGE(-) mice [ $20.2 \pm 2.2$  and  $32 \pm 4.5$  vs  $9.4 \pm 1.4$ , Figure 4(C)].

To investigate vascular changes, we performed an immunohistochemical study for CD31 [Figure 4(A)]. In PBS-treated mice, no CD31-positive vessels were observed in the submesothelial layer. The CG+3,4-DGE(-) mice showed increased CD31-positive vessels in the compact zone, an increase that was further augmented in 38  $\mu\text{mol/L}$  and 145  $\mu\text{mol/L}$  CG+3,4-DGE mice.



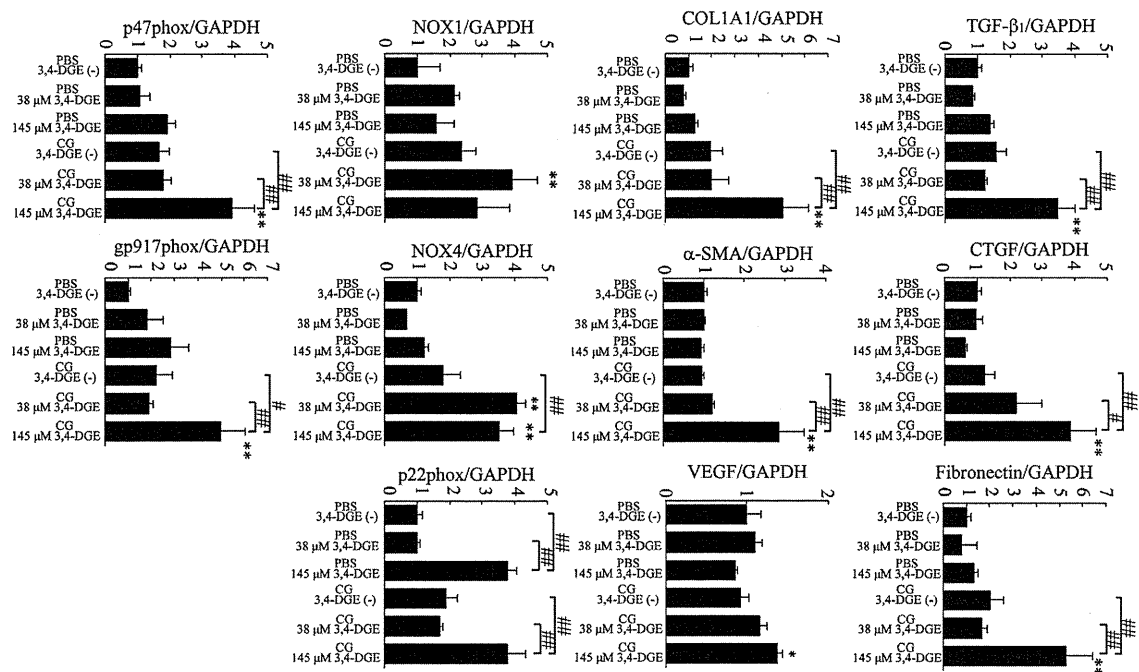


Figure 3 — Analysis by real-time reverse-transcriptase polymerase chain reaction of peritoneal expression of messenger RNA for transforming growth factor  $\beta 1$  (TGF- $\beta 1$ ), connective tissue growth factor (CTGF), fibronectin, collagen type 1  $\alpha 1$  (COL1A1), alpha smooth muscle actin ( $\alpha$ -SMA), vascular endothelial growth factor 164 (VEGF164), NOX1, NOX4, p22phox, p47phox, and gp91phox. GAPDH was used as a control. Number of mice: phosphate buffered saline (PBS) without 3,4-dideoxyglucosone-3-ene (3,4-DGE) ( $n = 7$ ); PBS+38  $\mu\text{mol/L}$  3,4-DGE ( $n = 5$ ); PBS+145  $\mu\text{mol/L}$  3,4-DGE ( $n = 5$ ); CG without 3,4-DGE ( $n = 5$ ); CG+38  $\mu\text{mol/L}$  3,4-DGE ( $n = 6$ ); and CG+145  $\mu\text{mol/L}$  3,4-DGE ( $n = 5$ ). All values: mean  $\pm$  standard error of the mean. \*  $p < 0.05$ ; \*\*  $p < 0.01$  versus mice receiving PBS with the same dose of 3,4-DGE; #  $p < 0.05$ ; ##  $p < 0.01$ .

The area of CD31-positive vessels in the submesothelial compact zone was also quantified [Figure 4(D)]. The area of these blood vessels was greater in 38  $\mu\text{mol/L}$  and 145  $\mu\text{mol/L}$  CG+3,4-DGE mice than in CG+3,4-DGE(–) mice, and the effect was dose-dependent ( $1.8\% \pm 0.45\%$  and  $8.3\% \pm 1.9\%$  vs  $0.42\% \pm 0.11\%$ ). These results demonstrate that 3,4-DGE can increase CD31-positive vessels in injured peritoneum.

We next examined the presence of mesothelial cells by cyokeratin staining. All PBS-treated mice, including those receiving 145  $\mu\text{mol/L}$  3,4-DGE showed almost intact mesothelial cells [Figure 4(A)]. Although CG+3,4-DGE(–) mice showed no change in mesothelial cells, mice treated with of 3,4-DGE in addition to CG showed severe detachment of mesothelial cells from the peritoneal membrane [Figure 4(A)].

#### APOPTOSIS

We next used TUNEL staining to examine apoptosis in peritoneal injury. Almost no apoptotic cells were detected without 3,4-DGE or with 38  $\mu\text{mol/L}$  3,4-DGE even in CG-treated mice. In CG+3,4-DGE(–) mice, apoptotic cells

were increased only in the abdominal rectus muscles, not in the submesothelial compact zone [Figure 5(A)]. The PBS+145  $\mu\text{mol/L}$  3,4-DGE and CG+145  $\mu\text{mol/L}$  3,4-DGE mice both showed pronounced apoptotic cells in peritoneum [Figure 5(A)].

For nuclear staining, DAPI was used. Most TUNEL-positive cells were also positive for DAPI, confirming that the TUNEL signals derived specifically from nuclei. The mean number of TUNEL-positive cells in PBS+3,4-DGE and CG+3,4-DGE mice was 3.0 and 5.9, respectively [Figure 5(B)], indicating that 3,4-DGE is relevant to apoptosis *in vivo* in the peritoneum.

To detect the cell type of the apoptotic cells, triple staining for TUNEL, DAPI, and CD45 (a leukocyte marker) was performed in CG+3,4-DGE mice [Figure 5(C)]. Some TUNEL-positive cells were positive for CD45, indicating that some of apoptotic cells were leukocytes.

#### ELIMINATION OF 3,4-DGE FROM THE PERITONEAL CAVITY AND APPEARANCE OF 3,4-DGE IN PLASMA

We next examined the rate at which 3,4-DGE was eliminated from the peritoneal cavity in PBS- or CG-treated



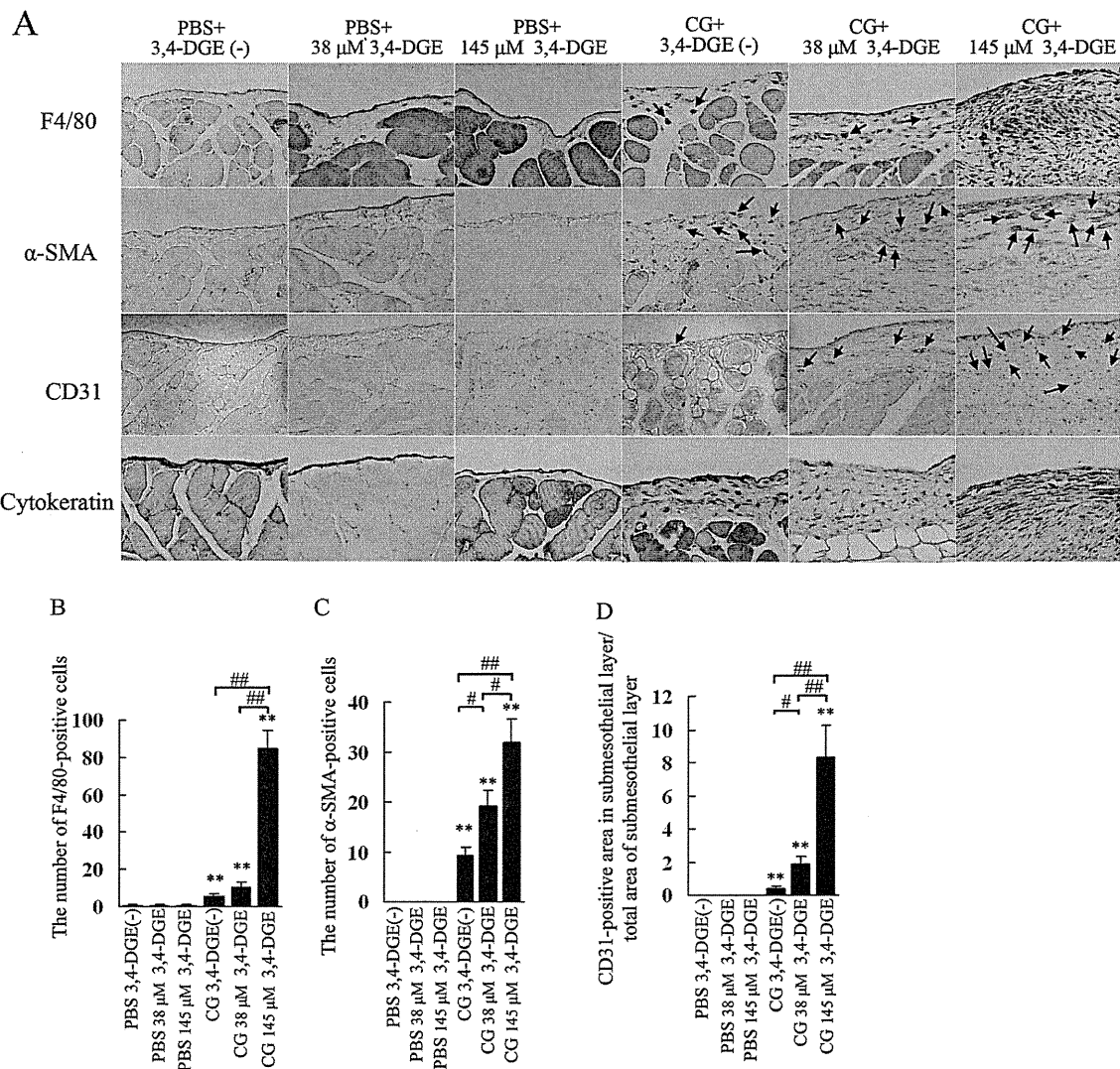


Figure 4 — (A) Immunohistochemical study for F4/80, alpha smooth muscle actin ( $\alpha$ -SMA), CD31, and cytokeratin in the peritoneum. Mice receiving chlorhexidine gluconate (CG) plus 38  $\mu$ M/L or 145  $\mu$ M/L 3,4-dideoxyglucosone-3-ene (3,4-DGE) showed increased F4/80-positive cells (arrows) and  $\alpha$ -SMA positive cells (arrows). Vessels positive for CD31 were increased in mice treated with CG plus 38  $\mu$ M/L or 145  $\mu$ M/L 3,4-DGE. Cytokeratin staining showed that mesothelial cells were detached in mice treated with CG plus 38  $\mu$ M/L or 145  $\mu$ M/L 3,4-DGE. (B) Number of F4/80-positive cells in the submesothelial area. (C) Number of  $\alpha$ -SMA-positive cells in the submesothelial area. (D) Ratio of the area in the submesothelial layer positive for CD31 to the total area of the submesothelial layer. Number of mice: phosphate buffered saline (PBS) without 3,4-DGE [PBS+3,4-DGE(-),  $n = 7$ ]; PBS+38  $\mu$ M/L 3,4-DGE ( $n = 5$ ); PBS+145  $\mu$ M/L 3,4-DGE ( $n = 5$ ); CG+3,4-DGE(-) ( $n = 5$ ); CG+38  $\mu$ M/L 3,4-DGE ( $n = 6$ ); CG+145  $\mu$ M/L 3,4-DGE ( $n = 5$ ). All values: mean  $\pm$  standard error of the mean. \*  $p < 0.05$ ; \*\*  $p < 0.01$  versus mice treated with PBS and the same dose of 3,4-DGE; #  $p < 0.05$ ; ##  $p < 0.01$ .

mice, because apoptosis was not detected in the 38  $\mu$ M/L 3,4-DGE group, a result that is not consistent with a previous *in vitro* study that showed induction of mesothelial cell apoptosis even in the presence of 38  $\mu$ M/L 3,4-DGE.

We speculated that the 3,4-DGE injected into the peritoneal cavity was rapidly eliminated, especially in injured perineum. The residual concentration of

3,4-DGE in PBS-treated mice was 53% [Figure 6(A)]. In contrast, CG-treated mice showed a much reduced residual level of 3,4-DGE [10%, Figure 6(A)]. Interestingly, in mice given 145  $\mu$ M/L 3,4-DGE, the plasma concentration of 3,4-DGE was much higher in the CG-treated group than in the PBS-treated group [Figure 6(B)]. These results indicate that injured peritoneum causes 3,4-DGE to disappear from the peritoneal

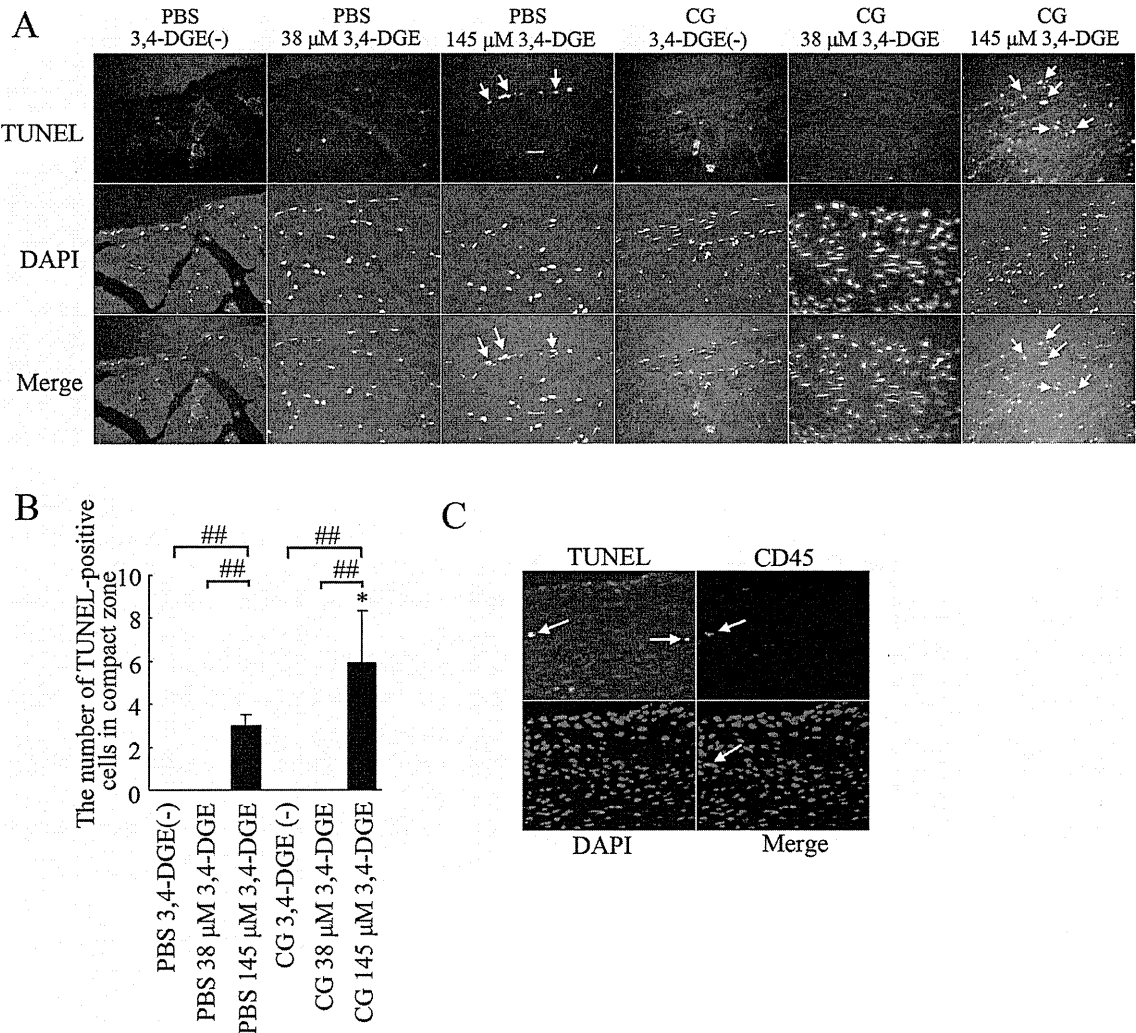


Figure 5 — Apoptotic cells in the peritoneum. (A) TUNEL staining (green), DAPI staining (blue), and merged images. Mice treated with phosphate-buffered saline (PBS) plus 145  $\mu$ mol/L 3,4-dideoxyglucosone-3-ene (3,4-DGE) showed TUNEL-positive cells (arrows). Mice treated with chlorhexidine gluconate (CG) plus 145  $\mu$ mol/L 3,4-DGE showed more TUNEL-positive cells than did mice treated with PBS+145  $\mu$ mol/L 3,4-DGE (arrows). DAPI was used as nuclear staining. Most TUNEL-positive cells were also positive for DAPI. Number of mice: PBS without 3,4-DGE [PBS+3,4-DGE(-),  $n = 7$ ]; PBS+38  $\mu$ mol/L 3,4-DGE ( $n = 5$ ); PBS+145  $\mu$ mol/L 3,4-DGE ( $n = 5$ ); CG+3,4-DGE(-) ( $n = 5$ ); CG+38  $\mu$ mol/L 3,4-DGE ( $n = 6$ ); CG+145  $\mu$ mol/L 3,4-DGE ( $n = 5$ ). (B) Ratio of TUNEL-positive cells to DAPI-positive cells in the submesothelial area in mice. All values: mean  $\pm$  standard error of the mean. \*  $p < 0.05$  versus mice treated with PBS and the same dose of 3,4-DGE; ##  $p < 0.01$ . (C) Triple staining for TUNEL (green), CD45 (red), and DAPI (blue) in mice ( $n = 5$ ) treated with CG+145  $\mu$ mol/L 3,4-DGE. Some of TUNEL-positive cells are leukocytes (arrows).

cavity rapidly and that some 3,4-DGE is absorbed into the systemic circulation.

MODIFIED PERITONEAL EQUILIBRATION TEST

Peritoneal equilibration tests were performed to examine the functional role of 3,4-DGE in peritoneal fibrosis. Figure 7(A) shows that the dialysate-to-plasma ratio of creatinine (D/P Cr) in PBS+38  $\mu$ mol/L 3,4-DGE mice was not different from that in PBS+3,4-DGE(-)

mice. In contrast, the D/P Cr was significantly higher in CG+38  $\mu$ mol/L 3,4-DGE mice than in PBS+38  $\mu$ mol/L 3,4-DGE or CG+3,4-DGE(-) mice (0.68 vs 0.55 and 0.54 respectively). By analyzing the ratio of net ultrafiltration to body weight, CG-treated mice not receiving 3,4-DGE showed reduced ultrafiltration and CG+38  $\mu$ mol/L 3,4-DGE mice showed net ultrafiltration failure. The MTAC urea also indicated that, compared with PBS+38  $\mu$ mol/L 3,4-DGE mice, CG+3,4-DGE mice showed increased urea transport. These results suggest that

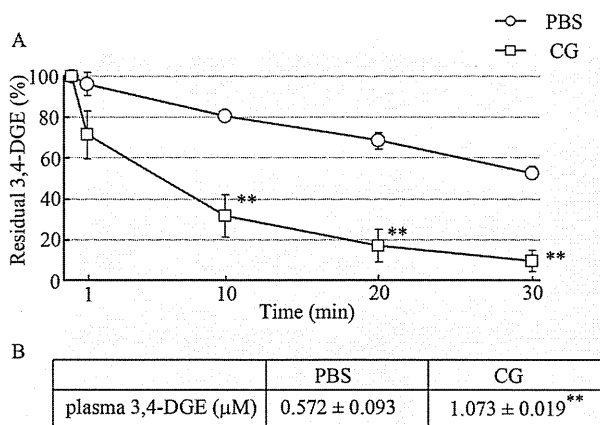


Figure 6 — Elimination rate of 3,4-dideoxyglucosone-3-ene (3,4-DGE) from the peritoneal cavity and appearance rate of 3,4-DGE in plasma. Mice were treated with phosphate buffered saline (PBS) or chlorhexidine gluconate (CG) 3 times in 1 week, and then 4 mL 3,4-DGE-containing PBS was injected into the peritoneal cavity. Peritoneal fluid was collected at 1, 10, 20, and 30 minutes after injection. (A) Residual concentration of 3,4-DGE in peritoneal fluid. Mice treated with CG showed rapid elimination of 3,4-DGE from the peritoneal cavity (PBS-treated:  $n = 8$ ; CG-treated:  $n = 7$ ). (B) Plasma level of 3,4-DGE in PBS- or CG-treated mice at 30 minutes after injection of 145 μmol/L 3,4-DGE. Compared with PBS-treated mice, those treated with CG showed high plasma levels of 3,4-DGE (PBS-treated:  $n = 2$ ; CG-treated:  $n = 3$ ). \*\*  $p < 0.01$  versus PBS-treated mice.

3,4-DGE is associated with high peritoneal transport in peritoneal fibrosis.

## DISCUSSION

Although previous reports showed that GDP-containing conventional PD solutions induce peritoneal fibrosis with enhanced peritoneal permeability even after 5 weeks *in vivo* (21), it is not clear whether 3,4-DGE is the sole cause of peritoneal changes. In the present study, we infused 3,4-DGE dissolved in PBS into the peritoneal cavities of mice to examine the effects of that compound on peritoneal fibrosis. Although there is some controversy about the use of CG to induce an encapsulating peritoneal sclerosis model (22), we used this existing model of CG-induced peritoneal injury to investigate the role of 3,4-DGE. Vlijm *et al.* reported that the condition of chronic renal failure can be a “first hit” in peritoneal damage and that perhaps other stimuli can substitute for CG in damaging mesothelial cells (22). Infusion of 3,4-DGE alone did not induce peritoneal changes in conditions of uninjured peritoneum. The peritoneal damage caused by 3,4-DGE alone may be different from that caused by PD solution because of the difference of glucose concentration. The combination of CG and 3,4-DGE caused thickening of the submesothelial zone, suggesting that 3,4-DGE is an aggravating

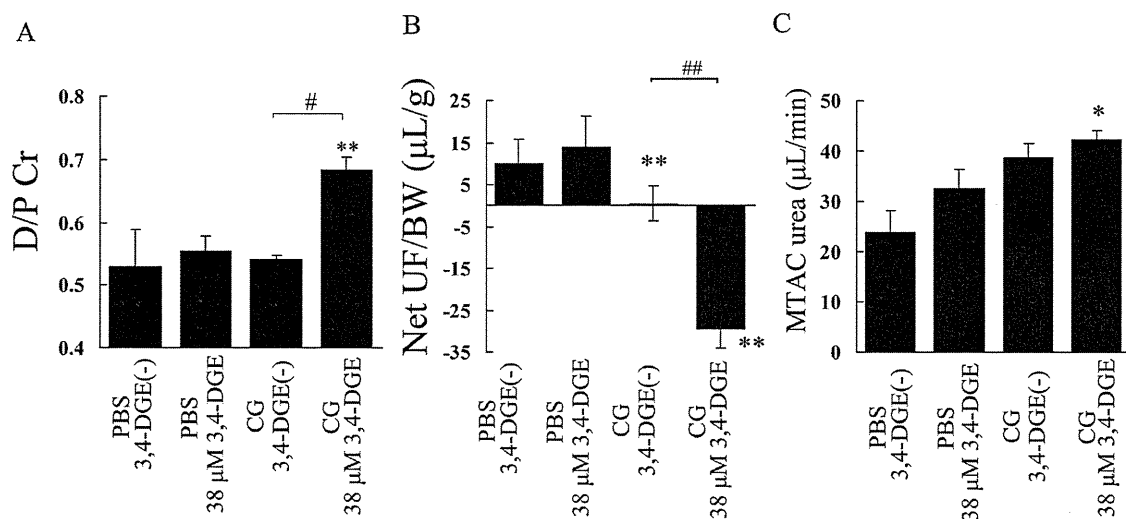


Figure 7 — Modified peritoneal equilibration test. (A) The creatinine (Cr) concentration in 7% glucose dialysate effluent (D) divided by the Cr concentration in plasma (P) in mice at 2 hours. (B) Net ultrafiltration (UF) / body weight (BW). (C) Mass transfer-area coefficient (MTAC). Compared with mice treated with phosphate buffered saline (PBS) plus 38 μmol/L 3,4-dideoxyglucosone-3-ene (3,4-DGE), mice treated with chlorhexidine gluconate (CG) plus 38 μmol/L 3,4-DGE showed high peritoneal transport. Net UF / BW and MTAC urea indicated that CG treatment induced ultrafiltration failure and high urea transport. Number of mice: PBS without 3,4-DGE [PBS+3,4-DGE(-),  $n = 3$ ]; PBS+38 μmol/L 3,4-DGE ( $n = 3$ ); CG+3,4-DGE(-) ( $n = 3$ ); CG+38 μmol/L 3,4-DGE ( $n = 5$ ). All values: mean ± standard error of the mean. \*  $p < 0.05$ ; \*\*  $p < 0.01$  versus PBS-treated mice receiving the same dose of 3,4-DGE; #  $p < 0.05$ ; ##  $p < 0.01$ .

factor in peritoneal fibrosis when peritoneal damage is already present.

The infusion of GDP-containing conventional dialysis solution with lipopolysaccharide induces a high peritoneal transport rate, with mild thickening of the peritoneal membrane (12). In the present study, we used 38  $\mu\text{mol/L}$  or 145  $\mu\text{mol/L}$  3,4-DGE-containing PBS. The 3,4-DGE alone did not elicit peritoneal fibrosis, probably because half the 3,4-DGE is eliminated from the peritoneal cavity at 30 minutes. In peritoneal mesothelial cells, VEGF-A, which enhances vascular permeability and angiogenesis, has been shown to be increased by MGO and 3,4-DGE (23,24). Blockade of VEGF by anti-VEGF monoclonal antibody prevents hyperglycemia-induced structural and functional peritoneal microvascular alterations in rats, indicating that VEGF plays a role in permeability to small molecules and angiogenesis (25). The present study shows that only CG+145  $\mu\text{mol/L}$  3,4-DGE mice showed increased levels of VEGF, leading to high peritoneal permeability as indicated by peritoneal equilibration tests. Antiangiogenic reagents TNP-470 and endostatin have been shown to ameliorate peritoneal fibrosis and permeability (26,27). In the present study, increased numbers of CD31-positive vessels were most often noted in CG+145  $\mu\text{mol/L}$  3,4-DGE mice, which is consistent with increased peritoneal permeability.

Expression of genes associated with extracellular matrix (TGF- $\beta$ 1, CTGF, fibronectin, and COL1A1) was significantly increased in the peritoneum of CG+145  $\mu\text{mol/L}$  3,4-DGE mice. In cultured human peritoneal mesothelial cells, stimulation with 3,4-DGE has been shown to increase TGF- $\beta$  secretion (24). Our study indicates that administration of 3,4-DGE without CG did not upregulate TGF- $\beta$ 1 mRNA expression. Taken together, these findings suggest that injured peritoneum expresses increased TGF- $\beta$  mRNA because of stimulation by 3,4-DGE.

Although the precise mechanism of upregulated TGF- $\beta$  expression in CG+145  $\mu\text{mol/L}$  3,4-DGE mice is not clear, we speculate that oxidative stress is one factor affecting TGF- $\beta$  expression in our model. Reduction of oxidative stress with L-2-oxothiazolidine-4-carboxylic acid (28), a glutathione precursor, or N-tert-butyl- $\alpha$ -phenylnitrone (29) lowered the TGF- $\beta$  level in cultured mesothelial cells, indicating that, in peritoneal mesothelial cells, oxidative stress can increase TGF- $\beta$ , which is one of the well-known inducers of EMT in mesothelial cells (30,31). Epithelial-mesenchymal transition is characterized by downregulation of E-cadherin and cytoskeletal rearrangement with expression of  $\alpha$ -SMA. Our results show that the number of  $\alpha$ -SMA-positive cells

was increased in the submesothelial zone. Although CG treatment alone or CG plus 38  $\mu\text{mol/L}$  3,4-DGE increased  $\alpha$ -SMA-positive cells, mRNA expression of  $\alpha$ -SMA in those groups of mice was not increased. Further investigation is needed into this discrepancy between mRNA and protein levels.

Oxidative stress is a key factor in the development of peritoneal fibrosis. Reactive oxygen species produced after stimulation with high glucose upregulate fibronectin expression through the protein kinase C pathway in human peritoneal mesothelial cells (32). Reactive oxygen species have been shown to play a role in changes of peritoneal membrane structure and function *in vivo*, and antioxidant prevents those changes (33). We showed upregulation of NOX4 and p47phox mRNA expression in CG+145  $\mu\text{mol/L}$  3,4-DGE mice compared with CG+3,4-DGE(-) mice. Macrophage infiltration was documented in the peritoneum of 38  $\mu\text{mol/L}$  or 145  $\mu\text{mol/L}$  CG+3,4-DGE mice. The infiltrating macrophages aggravate peritoneal fibrosis by secreting profibrogenic cytokines (34). Peritoneal macrophage infiltration is an independent predictor of baseline peritoneal permeability in PD patients (35). At 38  $\mu\text{mol/L}$  3,4-DGE can influence macrophage infiltration and vessel formation.

Conventional PD solutions and GDPs induce apoptosis in mesothelial cells. High concentrations of 3-deoxyglucosone or MGO induce mesothelial cell apoptosis (36,37). Administration of 3,4-DGE within the concentration range seen in conventional PD solutions induces apoptosis in cultured mesothelial cells through caspase- and Bax-dependent pathways (10,38), suggesting that 3,4-DGE mediates, at least in part, the cytotoxicity of conventional PD solutions. The precise mechanism and role of apoptosis in the peritoneum *in vivo* needs further investigation. We showed that 145  $\mu\text{mol/L}$  3,4-DGE in combination with CG induced cell apoptosis in the thickened peritoneal compact zone *in vivo*. As previously reported (39), some of the apoptotic cells were leukocytes. The inability of 38  $\mu\text{mol/L}$  3,4-DGE to induce apoptosis might be a result of rapid elimination of 3,4-DGE from peritoneal cavity. Peritoneum injured by CG can accelerate that process, elevating plasma levels of 3,4-DGE.

## CONCLUSIONS

Our study shows that, when mild peritoneal damage is already present, 3,4-DGE enhances peritoneal injury by augmenting macrophage infiltration and extracellular matrix deposition. These findings help to elucidate the effect of 3,4-DGE in peritoneal fibrosis *in vivo*.